Published in final edited form as:
J Alzheimers Dis. 2009 July ; 17(3): 553–570. doi:10.3233/JAD-2009-1074.

Testing the Neurovascular Hypothesis of Alzheimer's Disease: LRP-1 Antisense Reduces Blood-Brain Barrier Clearance, Increases Brain Levels of Amyloid-*β* Protein, and Impairs Cognition

Laura B. Jaeger[a,b], **Shinya Dohgu**[b,c], **Mark C. Hwang**[b,c], **Susan A. Farr**[b,c], **M. Paul Murphy**[d], **Melissa A. Fleegal-DeMotta**[b,c], **Jessica L. Lynch**[b,c], **Sandra M. Robinson**[b,c], **Michael L. Niehoff**[b,c], **Steven N. Johnson**[b,c], **Vijaya B. Kumar**[b,c], and **William A. Banks**[a,b,c,*]

[a]Department of Pharmacological and Physiological Science, Saint Louis University School of Medicine, St. Louis, MO, USA

[b]Geriatric Research Education and Clinical Center (GRECC), VA Medical Center, St. Louis, MO, USA

[c]Department of Internal Medicine, Division of Geriatric Medicine, Saint Louis University School of Medicine, St. Louis, MO, USA

[d]Department of Molecular and Cellular Biochemistry, University of Kentucky, Lexington, KY, USA

Abstract

Decreased clearance is the main reason amyloid-*β* protein (A*β*) in increased in the brains of patients with Alzheimer's disease (AD). The neurovascular hypothesis states that this decreased clearance is caused by impairment of low density lipoprotein receptor related protein-1 (LRP-1), the major brain-to-blood transporter of A*β* at the blood-brain barrier (BBB). As deletion of the LRP-1 gene is a lethal mutation, we tested the neurovascular hypothesis by developing a cocktail of phosphorothioate antisenses directed against LRP-1 mRNA. We found these antisenses in comparison to random antisense selectively decreased LRP-1 expression, reduced BBB clearance of Aβ_{42}, increased brain levels of Aβ_{42}, and impaired learning ability and recognition memory in mice. These results support dysfunction of LRP-1 at the BBB as a mechanism by which brain levels of A*β* could increase and AD would be promoted.

Keywords

Alzheimer's disease; antisense; blood-brain barrier; cognition; learning; low density lipoprotein receptor related protein-1 (LRP-1); memory; transporter

INTRODUCTION

Alzheimer's disease (AD) is the most common cause of dementia among people over the age of 65 [1]. It is a progressive disease characterized by extensive cortical and hippocampal neurodegeneration. The AD brain is distinguished by the presence of amyloid plaques

*Corresponding author: William A. Banks, MD, VAMC, 915 N. Grand Blvd, St. Louis, MO 63106, USA. Tel.: +1 314 289 7084; Fax: +1 314 289 6374; bankswa@slu.edu.

comprised partly of insoluble extracellular deposits of amyloid-β protein (Aβ) [2]. Aβ is produced when amyloid-β protein precursor (AβPP) is cleaved by the β- and γ-secretase enzymes. The most common Aβ isoform is 40 amino acids long (Aβ_{40}) [3]. The 42 amino acid isoform (Aβ_{42}), however, demonstrates a higher degree of neurotoxicity, a characteristic that may be due to its propensity to form insoluble aggregates [4–6]. Previous studies have shown that deposits of Aβ in the brain parenchyma of AD patients consist of mainly Aβ_{42}; therefore, this isoform is though to play a major role in AD pathology [7].

Although most animal models of AD are based on mutations that result in the overexpression of AβPP [8], only the rare (< 1% of all cases) autosomal dominant form of AD is associated with increased production. The majority of AD cases occur sporadically after the age of 60 (late onset AD, LOAD) and are not associated with overproduction of Aβ, but by its altered clearance. Altered rates of degradation by neprylisin, insulin-degrading enzyme, or endothelin-converting enzyme have been proposed as the primary mechanism for Aβ removal from the brain [9]. However, Aβ is also removed from brain by being transported in the brain-to-blood direction by the blood-brain barrier (BBB). The vascular BBB is comprised of endothelial cells joined together by intercellular tight junctions that prevent the unregulated exchange of substances between the brain and the blood, thereby providing a “barrier” function. According to the neurovascular hypothesis of AD, decreased brain-to-blood transport of Aβ by these brain endothelial cells would lead to increased brain Aβ and thus contribute to AD [10].

Low density lipoprotein receptor-related protein-1 (LRP-1) is known to function as a BBB clearance (or efflux) transporter for Aβ. Efflux of Aβ is initiated when it binds directly to LRP-1 at the abluminal membrane of the brain endothelial cell [11]. Efflux of Aβ by LRP-1 is modulated by the apolipoproteins ApoE and ApoJ [12], and LRP-1 itself may naturally decline with age. Immunocytochemistry of brain microvessels from young (2 months) and old (9 months) C57BL/6 wild-type mice revealed that there is a 42% reduction in LRP-1 positive vessels in aged mice [13]. Further-more, a postmortem study of human AD patients indicates that LRP-1 levels are approximately two-fold lower in AD brains compared to the of age-matched controls [14]. Currently, no animal model exists for the study of the role of LRP-1 in AD because LRP-1 knock-out mice die at day 13.5 during embryonic development [15]. For the purpose of this project, we chose to use antisense oligodeoxynucleotides (ODNs) to alter expression of LRP-1 in mice so that we could directly test the neurovascular hypothesis *in vivo*.

To increase stability, we modified the ODN by synthesizing them with a phorophorthioate backbone (PS-ODN) [6]. Our previous work has shown that PS-ODN are transported across the BBB by a saturable transporter [6,16–19]. This work also indicates that a “cocktail” of PS-ODN directed at different targets within the mRNA is more effective than individual PS-ODNs [20]. Therefore, we synthesized two PS-ODNs directed at different regions of the LRP mRNA and administered them together as an antisense cocktail. Here, we found that the cocktail PS-ODNs but not a random control PS-ODN, decreased LRP-1 expression in brain endothelial cells *in vitro* and *in vivo*, was selectively taken up by the hippocampus and largely retained by brain, selectively decreased brain-to-blood efflux *in vitro* and *in vivo* of radioactively labeled Aβ_{42}, increased endogenous brain levels of Aβ_{42} in mice treated with antisense, and impaired learning and memory. Overall, these results strongly support the neurovascular hypothesis of AD in that decreased expression and function of LRP-1 leads to Aβ accumulation in brain and impaired cognition.

MATERIAL AND METHODS

Animals

Male CD-1 mice (>8 weeks old; weighing 30–35 g) were used (Charles River, Wilmington, MA) in all experiments. The mice were maintained in a temperature-controlled (19–23°C) room on a 12:12 h light-dark cycle (lights on at 0600 h) with experiments conducted during the light phase. All procedures were in accordance with the NIH Guidelines for the Care and Use of Laboratory Animals and were approved by the Veterans Affairs – Saint Louis Animal Care Committee.

Synthesis of PS-ODNs

PS-ODNs were synthesized by the Midland Certified Reagent Company (Midland, TX). The sequences of the three PS-ODNs used in these studies are:

19mer (Anti-LRP1): 5′-(_P=S)TGATTTGGTCTCTGCAGGC-3′

23mer (Anti-LRP1): 5′-(_P=S)GTGTGGGCCGATGCAAACAGCAG-3′

21mer (Random): 5′-(_P=S)GAGAAGGTTGTGTGATCTTCA.

The 23mer (nt 442–418) was designed to bind to the translation start site and the 19mer (nt 559–541) to an LRP-1 coding region based on the National Center for Biotechnology Information (NCBI) GenBank accession number NM_008512. Except where noted, the 19mer and 23mer PS-ODNs were administered simultaneously as a cocktail in equal amounts (e.g., 5 μg of 19mer + 5 μg of 23mer = 10 μg total antisense). The 21 mer PS-ODN was designed as control sequence (“random”) by randomly picking letters from the two sequences used to construct the 19mer and 23mer PS-ODNs and is the average length of the two PS-ODNs that compose the cocktail. A check of the NCBI mouse nucleotide Basic Alignment Search Tool (BLAST) database showed that this random antisense did not share sequence homology with any mouse genes. The lyophilized PS-ODNs were dissolved in 09% NaCl at a concentration of 1 mg/ml and stored at −70°C until use.

Reagents

Lyophilized 42 amino acid murine Aβ (Aβ_{42}; Bachem AG, Switzerland was solubilized at a concentration of 1 mg/ml in 0.1% NH_4OH and stored at −70°C until use. All other reagents were purchased from Sigma (Sigma-Aldrich, St. Louis, MO) unless otherwise specified.

Iodination (Aβ_{42} and RAP)

Murine Aβ_{42} was radioactively labeled with the chloramine-T method [21]. Chloramine T (1 mg/ml) and sodium metabisulfite (10 mg/ml) were dissolved in 0.25 M chloride-free sodium phosphate buffer (PB) containing 0.25 M NaH_2PO_4 + 0.25 M Na_2HPO_4, pH = 7.5. Two mCi of ^{131}I (Perkin Elmer, Boston, MA), 5 μg of peptide [either Aβ_{42} or receptor-associated protein (RAP)], and 10 μl of chloramine-T were mixed and after 60 sec 10 μl of sodium metabisulfite was added to halt the reaction. The iodinated material (I-Aβ_{42}) was purified by eluting with 100 μl aliquots of PB on a G-10 Sephadex column. The level of radioactivity in each eluted fraction was determined in a Wallac Wizard gamma counter (EG & G Wallac, Turku, Finland). The two fractions that corresponded to the monoiodinated compound were identified by elution position and peak in radioactivity. The integrity of the radioactive label for these two fractions was confirmed by precipitation with 30% trichloroacetic acid (TCA) and was greater than 95%. I-Aβ was stored at −07°C and used within 48 h of radioactive labeling.

Label With ^{32}P (Ps-Odns)

This method has been described previously [20]. Briefly, PS-ODNs were end-labeled by mixing 1–10 μg of PS-ODN with 1.5 μl of 10x kinase buffer, 1.5 μl of T4 Polynucleotide Kinase (New England Biolabs, Ipswich, MA) and 10 μl of [γ^{32}P] ATP (Perkin Elmer, Boston, MA). The mixture was incubated in a 37°C water bath for 45 min. The kinase was heat inactivated by incubating the sample in a heat block set to 65°C for 5 min. Labeled oligonucleotide (P-Olg) was removed from the reaction mixture by ethanol precipitation followed by centrifugation. For the initial ethanol precipitation, the labeled PS-ODN was mixed with 80 μl of distilled water (dH_2O), 10 μl 30 M Na-acetate (pH = 5.0), 2–5 μl of Pellet Paint Co-Precipitant (Novagen, Madison, WI) and 300 μl of cold ethanol. This mixture was then subjected to an overnight incubation in a −70°C freezer. The next day, P-Olg was separated from the mixture by centrifugation at 13,000 rpm for 20 min. After removing the supernatant, the pellet (containing the P-Olg) was resuspended in 500 μl of cold ethanol and centrifuged at 13,000 rpm for 15 min 4 times. After the final wash, the pellet was resuspended in 100 μl of dH_2O and the level of radioactivity determined. P-Olgs (P-19mer or P-23mer) were stored at −70°C and used within 48 h.

METHODS FOR ACUTE ANTISENSE ADMINISTRATION STUDIES

Isolation of mouse brain microvascular endothelial cells (BMECs)

BMECs were isolated using a modified method of Szabó et al. [22]. In brief, cerebral cortices from 8-weed-old CD-1 mice were isolated, cleaned of meninges, and minced. The homogenate was digested with collagenase type II (1 mg/mL) and DNase I (30 U/mL) in Dulbecco's Modified Eagle Media (DMEM) [containing 100 units/mL penicillin, 100 μg/mL streptomycin, 50 μg/mL gentamicin and 2mM GlutaMAX-I (Invitrogen, Carlsbad, CA)] at 37°C for 40 min. After digestion, 20% bovine serum albumin (BSA) dissolved in DMEM was added, the sample centrifuged at, 1,000 × g for 20 min, the supernatant containing the neurons and glial cells removed, and the pellet containing the microvessels further disgested at 37°C for 30 min with collagenase/dispase at a concentration of 1 mg/mL (Roche, Mannheim, Germany) and DNase I (30 U/mL dissolved in DMEM). After the second enzyme digestion, we then layered the pellet on a 33% Percoll (Amersham Biosciences, Piscataway, NJ) gradient and centrifuged at 1,000 × g for 10 min to separate the microvessels. To create the Percoll gradient, 33% Percoll solution (8 mL Percoll, 14.4 mL phosphate buffered saline (PBS), 0.8 mL plasma derived serum (PDS), and 0.8 mL 10X PBS) was centrifuged at 20,300 × g for 1 h. After the centrifugation, a layer of microvessels was formed in the middle of the Percoll gradient, above the red blood cell layer. Microvessels were washed by resuspension in DMEM and centrifuged at 1,000 × g for 10 min. The microvessel pellet was dissolved in DMEM and the mix seeded on culture dishes previously coated with a coating buffer (0.05 mg/mL fibronectin, 0.05 mg/mL collagen I and 0.1 mg/mL collagen IV) and allowed to dry. The freshly seeded cells were incubated at 37°C for 24 h in a humidified atmosphere of 5% CO_2/95% air in a 1:1 mixture of DMEM and Ham's F12 Nutrient Mixture (DMEM/F-12) that had been supplemented with 20% plasma-derived bovine serum (Quad Five, Ryegate, MT), 100 units/mL penicillin, 100 μg/mL streptomycin, 50 μmL gentamicin, 2 mM GlutaMAX-I and 1 ng/mL basic fibroblast growth factor (bFGF). By the next day, the BMECs had migrated from the isolated capillaries and started to form a continuous monlayer. To eliminate pericytes, glial cells, and other contaminating cells, BMECs were treated with puromycin (4 μg/mL) for the first 2 days of culture [23]. Culture media was changed every other day and BMECs had reached 80–90% confluency by day 7.

Culture of BMECs on Transwell inserts

BMECs were seeded (4×10^4 cells/insert) on a fibronectin-collagen IV (0.1 and 0.5 mg/mL, respectively)-coated polyester membrane (0.33 cm^2, 0.4 μm pore size) inside of a Transwell-

Clear insert (Costar, Corning, NY) and the inserts placed (one per well) in 24-well culture plates (Costar). Cells were cultured in DMEM/F-12 media that was supplemented with 20% PDS, 100 units/mL penicillin, 100 μg/mL streptomycin, 50 μg/mL gentamicin, 2 mM GlutaMAX-I, 1 ng/mL bFGF and 500 nM hydrocortisone. Cultures were maintained at 37°C with a humidified atmosphere of 5% CO_2/95% air until the BMEC monolayers reached confluencey (about 3 days). The integrity of the BMEC monolayers was tested by measuring transendothelial electrical resistance (TEER). TEER measurements were taken before the experiments using an EVOM Epithelial Tissue Voltohmmeter equipped with an STX-2 electrode (World Precision Instruments, Sarasota, FL).

Transport of I-Aβ_{42} in BMEC cultures

For the transendothelial transport experiments, the media was first removed from all wells and the BMECs washed with a physiological buffer (141 mM NaCl, 4.0 mM KCl, 2.8 mM $CaCl_2$, 1.0 mM $MgSO_4$, 1.0 mM NaH_2PO_4, 10 mM HEPES, 10 mM D-glucose, pH 7.4) containing 1% BSA. Physiological buffer was added to the luminal (0.1 mL) and abluminal (0.6 mL) chambers of the Transwell insert. For the purpose of this experiment, I-Aβ_{42} (1×10^6 cpm/mL) was loaded into the abluminal chamber and the luminal chamber served as the collecting chamber. The sampling volume for the luminal chamber was 90 μL.

To quantify I-Aμ_{42} efflux, collecting chambers were sampled at various time points (10, 20, 40, and 60 min) with volume replacement with fresh physiological buffer (supplemented with 1% BSA). All sample were mixed with 30% TCA (for a final concentration 15%) and centrifuged at 5,400 × g for 15 min at 4°C. The amount of radioactivity in the TCA precipitate was determined in a gamma counter. The permeability coefficient and clearance of TCA-precipitable I-Aβ_{42} was calculated by the method of Dehouck et al. [24]. Clearance was expressed as microliters (μL) of radioactivity diffusing from the abluminal to luminal chamber as calculated from the initial level of radioactivity in the abluminal chamber and final level of radioactivity in the collecting (or luminal) chamber as shown by the formula:

$$\text{Clearance}\ (\mu L) = [C]_C \times V_C / [C]_L$$

where $[C]_L$ is the initial level of radioactivity in the abluminal chamber (in cpm/μL), $[C]_C$ is the level of radioactivity in the luminal chamber (in cpm/μL) at any given time, and V_C is the volume of the collecting chamber (in μL). During the initial 60 min period of the experiment, the clearance volume increased linearly with time.

When the volume cleared from the abluminal chamber was plotted versus time, the slope of the clearance curve was estimated by linear regression analysis. The slope of the clearance curve for the BMEC monolayers is denoted as PS_{app}, where PS is the permeabilitysurface area product (in μL/min). The slope of the clearance curve in the absence of BMECs is denoted as $PS_{membrane}$. The actual PS value for the BMEC monolayers (PS_{trans}) was then calculated from the following formula:

$$1/PS_{app} = 1/PS_{membrane} + 1/PS_{trans}$$

PS_{trans} values were then divided by the surface area of the Transwell inserts (0.33 cm^2) to generate the permeability coefficient (P_{trans}, in cm/min).

The saturability of I-Aβ_{42} efflux was measured by adding unlabeled Aβ_{42} (1 μg/mL) to the loading chamber with the radiolabeled protein (1×10^6 cpm/mL). When the effect of antisense cocktail on I-Aβ_{42} efflux was examined, either the antisense cocktail or control random

antisense was dissolved in serum-free DMEM/F12 media. Cells were washed with serumfree medium and then exposed for 24 h to 1 μg/mL of cocktail or random antisense added into the luminal side of the chamber.

Isolation of mouse brain microvessels (MBMs)

MBMs were isolated by a modification of a method of Gerhart et al. [25]. All glassware was pre-coated with PBS supplemented with 1% BSA (% BSA/PBS). This was done to minimize adhesion and to maximize recovery of microvessels. Briefly, ten to twelve cerebral cortices from adult male CD-1 mice were collected and the meninges removed and homogenized on ice in 5 mL of cold stock buffer (25 mM HEPES, 1% dextran and 1 envelope of Minimum Essential Medium (Invitrogen), pH 7.4). The homogenate was filtered through a series of nylon mesh membranes (300 μm, then twice through 100 μm; Spectrum, Houston, TX), mixed with an equal volume of 40% dextran in stock buffer, and centrifuged at 3,000 × g for 30 min at 4° C. The supernatant with the lipid layer was removed and the pellet resuspended in stock buffer. The suspension was passed through a 25 μm nylon mesh membrane (Bio-Design, Carmel, NY). The microvessels on the surface of the membrane were washed with stock buffer four times, collected from the membrane, and then centrifuged at 3,000 × g for 30 min at 4°C, the supernatant discarded, and the microvessel pellets resuspended in incubation buffer (129 mM NaCl, 2.5 mM KCl, 7.4 mM Na_2PO_4, 1.3 mM KH_2PO_4, 0.63 mM $CaCl_2$, 0.74 mM $MgSO_4$, 5.3 mM glucose, 0.1 mM ascorbic acid, pH 7.4) until further use.

Immunohistochemistry of LRP-l in isolated MBMs

Isolated MBMs treated with either incubation buffer, random antisense, or antisense cocktail (10 μg/mL) in incubation buffer for 24 h were dropped onto glass slides and heat-fixed at 95° C for 10 min. They were fixed with 3.7% formaldehyde for 10 min at room temperature and permeabilized with 0.3% Triton X-100 in 1% BSA/PBS for 15 min at room temperature. Slides were treated with 10 μg/mL anti-LRP-1 antibody (H-80; Santa Cruz biotechnology, Santa Cruz, CA) in 1% BSA/PBS for an overnight incubation at 4°C, washed once with PBS, there times with balanced salt solution (130 mM NaCl, 5.4 mM KCl, 1.8 mM $CaCl_2$, 4 mM $MgCl_2$, 20 mM HEPES, 5.5 mM glucose, pH 7.4) and once with PBS. They were then incubated with 20 μg/mL Alexa Fluor 488-conjugated anti-rabbit IgG (Invitrogen) in 1% BSA/PBS for 1 h at room temperature. After washing, microvessels were covered with Vectashield Hard Set mounting medium (Vector Laboratories, Burlingame, CA) and coverslips applied. Fluorescence was datected with Zeiss Axiovert 40 CFL fluorescent microscope (Carl Zeiss, Inc., Thornwood, NY). Images were obtained from 5–6 microvessels in each group and mean fluorescent intensity was quantifield using Image J analysis software (National Institute of Health, USA).

Calculation of Ki and exposure time

Multiple-time regression analysis [26–28] was used to determine the rate of uptake of P-Olg from blood to brain. Brain/serum ratios calculated 2–30 min after i.v. injection were plotted against their respective exposure times (Expt). Expt is used instead of real time to correct for the clearance of the injected substance from the blood which would otherwise overestimate the influx rate. The slope of the linear portion of the brain/serum ratios vs Expt relation measures the unidirectional influx rate (Ki), while the y-intercept measures the initial volume of distribution (Vi) in the brain. Expt was calculated using the formula:

$$Expt = \left[\int_o^t C_p(t)\,dt\right] / C_p t$$

where *t* is time, C_P is the level of radioactivity in the serum and C_Pt is the level of radioactivity in the serum at time *t*.

Calculation of the percent uptake of dose

P-19mer or P-23mer (5×10^5 cpm) were injected into the jugular vein of mice in 0.2 ml of lactated Ringer's solution (LR; Baxter Healthcare Corporation, Deerfiled, IL) supplemented with 1% BSA (LR-BSA). Between 2–30 min after the iv injection, the brain or liver was removed, weighed, and the level of radioactivity measured. Whole blood collected from the carotid artery was centrifuged at 5000 × g for 15 min and the level of radioactivity in the serum determined. The % of the injected dose taken up by each gram of whole brain, brain region (hippocampus (HPC) or frontal cortex (FC)), or liver (% Inj dose/g tissue) was calculated from the formula:

$$\% \quad Inj \quad \text{dose}/g \quad \text{tissue} = 100\,(Am/Cpt - Vi)\,Cpt/Inj$$

where Am/Cpt represents the tissue/serum ratio at time *t* and Inj is the mean dose injected i.v. Subtracting Vi from the tissue/serum ratio corrects for P-Olg in the vascular space of the whole tissue. This removes the vascular contribution so that values represent only the P-Olg that has been taken up by tissue.

Measuring saturability of brain uptake for cocktail ODNs

To determine if brain uptake of each individual P-Olg was saturable, 10 μg/mouse of unlabeled cocktail PS-ODN (either 19mer or 23mer) was included in the i.v. injection of either P-19mer or P-23mer at a dose of 5×10^5 cpm/200 μ1 of LR-BSA. Brain and serum samples were collected 30 min after i.v. injection. Results were expressed as brain/serum ratios.

Capillary depletion

This method was performed to determine the distribution of the iv cocktail PS-ODNs between brain tissue and the brain capillaries [20,30]. Mice received an i.v. injection of either P-19mer or P-23mer at a dose of 5×10^5 cpm/200 μ1 LR-BSA into the jugular vein. Washout of the vascular space was performed to remove any substances that were intravascular or loosely adhered to the capillary lumen of the brain microvasculature. This method removes more than 95% of the blood from the brain.

Mice were anesthetized with 40% urethane 30 min after the i.v. injection of P-Olg, the abdomen opened, and arterial blood collected from the abdominal aorta. The thorax was opened with a midline sternal incision and the descending thoracic aorta was clamped. Both jugular veins were severed and an 18-gauge needle connected to a 20 ml syringe containing LR was inserted into the left ventricle of the heart. LR (20 ml) was infused into the mouse heart over a period of 1–2 min, washing out the vascular space of the brain. the brain was then removed, weighed, and placed in a glass homogenizer containing 0.8 ml of physiologic buffer (10 mM HEPES, 141 mM NaCl, 4 mM KCl, 2.8 mM $CaCl_2$, 1 mM $MgSO_4$, 1 mM NaH_2PO_4 and 10 mM D-glucose; this buffer was then adjusted to pH = 7.4). After 10 strokes with the pedestal, a quantity of 1.6 ml of the physiologic buffer containing 26% dextran was added to the homogenate. The homogenate was mixed and homogenized a second time (3 strokes). All homogenization steps were performed at 4°C on ice. The homogenate was centrifuged at 5400 × g for 15 min at 4° C in a swinging bucket rotor. supernatant (brain parenchyma) was separated from the pellet (brain microvasculature) and the levels of radioactivity determined. Results were expressed as the volume of distribution (V_D) in tissue (parenchyma or capillary)/serum ratios with the formula:

$$V_D = (cpm/\text{gram of tissue}) / (cpm/ml \quad \text{of serum})$$

Acute effects of i.v. antisense

In studies in which mice were treated acutely with i.v. antisense cocktail, mice received an injection into the tail vein of cocktail (7 μg each of 19mer and 23mer in 0.1 ml saline) or saline. The affects of antisense treatment on brain efflux of I-Aβ_{42} (5,000 cpm/μ1 LR-BSA) 4, 12, and 24 h later was determined.

In other studies, I-Aβ_{42} was administered by intracerebroventricular (i.c.v.) injection. Brains were collected at 0 and 10 min and the level of radioactivity was quantified with a gamma counter. Results were expressed as the log % of the injected dose of I-Aβ_{42} in brain (amount detected/amount injected * 100 = % Inj Dose) and plotted against time (min). The -slope of this line is reported as a measure of brain-to-blood efflux.

Quantitative real-time PCR (LRP-1 and RAGE mRNA)

RNA was isolated from hemibrain homogenates of mice treated with repeated i.v. saline, random, or cocktail antisense (7 μg/100 μ1) using the Qiagen RNeasy Lipid tissue mini kit protocol. Total cDNA was produced by reverse transcription using the Applied Biosystems Taqman reverse transcription system of 0.2 μl of purified RNA, 3 μl 10X RT buffer, 6.6 μl $MgCl_2$, 6 μl 2.5 mM dNTPs, 1.5 μl random hexamers, 0.6 μl Rnase inhibitor, and 0.75 μl Multiscribe RT. Samples were incubated for 10 min at 25°C, 30 min at 48°C, and 5 min at 95° C. Quantitative real-time PCR was performed in an Applied Biosystems 7300 Real-Time PCR System. Amplification was carried out in 25 μl reaction mixtures containing 1 μl of template cDNA, 0.5 μl of each 5 mm primer, 12.5 μl 2X SYBR green mastermix, and 10.5 μl PCR water. Cycling conditions were one cycle at 95°C for 10 min, followed by 50 cycles of 95°C for 15 s, and 60°C for 1 min followed by one cycle at 95°C for 15 s, 60°C for 15 s and 95°C for 15 s. Primers were made using Primer 3 software (Whitehead Institute for Biomedical Research) and primer efficiency was between 95–105%. Sequences were: RAGE forward 5′-ccctgagacgggactcttta, reverse 5′-gttggataggggctgtgttc; LRP-1 forward 5′-agtccacatgttccctaccg, reverse 5′-agagccaaggaaggaaagc and Beta Actin forward 5′-ttcctccctggagaagag, reverse 5′-tgccacaggattccatac. The relative amount of gene copies was extrapolated using the comparative Ct method with beta actin as a normalizer and Stratagene mouse standard RNA as a calibrator.

In vivo brain-to-blood efflux rate of i.c.v. antisense

A standard method was used to quantify brain-to-blood efflux rates [16,31]. Mice were anesthetized with i.p. urethane, the scalp removed, and a hole made through the cranium (1.0 mm lateral and 0.5 mm.posterior to bregma) with a 26-gauge needle. The entire needle, except 2.5 to 3.0 mm of the tip, was covered by PE-10 tubing, ensuring that the needle did not penetrate the floor of the ventricle.

A P-Olg (5×10^3 cpm/μl) was administered with a 1.0 μl Hamilton syringe. Mice were decapitated at 2, 5, 10, or 20 min after injection, the brain was removed and the level of radioactivity in the brain measured. The amount of radioactivity in the brain at $t = 0$ was estimated in mice overdosed with urethane. The log of % Inj Dose in each brain was plotted against time (min) and the slope determined by linear regression analysis.

In some experiments, mice received two i.c.v injections (antisense cocktail or saline i.c.v. and, at $t = 30$ min or $t = 24$ h, i.c.v. I-Aβ_{42}). In these cases, the dose of antisense given was 200 ng/μl LR-BSA and the dose of I-Aβ_{42} given was 5×10^3 cpm/μl LR-BSA.

In the specificity experiment, mice received two i.c.v. injections. The first injection consisted of either antisense cocktail, random antisense, antisense directed against AβPP, antisense directed against preproenkephalin (PPE), or saline at a dose of 1.0 μl LR-BSA. At t = 24 h, I-Aβ_{42} was given i.c.v. at a dose of 5×10^3 cpm/μl LR-BSA. Neuronal cells have been shown to metabolize Aβ *in vitro* by an LRP-dependent mechanism, however, the rate of this degradation is 50 to 100-fold slower than BBB efflux of Aβ *in vivo* [13]. Because of this, all data collected on the effects of acute centrally administered antisense cocktail on I-Aβ_{42} efflux was collected within 0–20 min after i.c.v. administration of I-Aβ_{42}.

METHODS FOR CHRONIC ANTISENSE ADMINISTRATION STUDIES

Chronic i.c.v. infusion of antisense

Mice were implanted with Alzet mini-osmotic pumps (DURECT Corporation,Cupertino, CA) fitted with a brain infusion assembly and containing saline or antisense or random antisense (200 ng/μl; rate; 0.5 μl/h). Prior to implantation, mice were anesthetized with isoflurane (Webster Veterinary Supply, Sterling, MA) and secured in a stereotaxic apparatus (David Kopf Instruments, Tujunga, CA). A subcutaneous (sc) pocket was then created from the scalp incision to the midscapular region on the back of the mouse by inserting a hemostat under the skin and then opening and closing the hemostat twice. This created a small tunnel under the skin into which the osmotic pump was inserted. A midline sagittal incision was made in the scalp and a hole was drilled through the skull for cannula implantation. Brain cannulas were stereotaxically inserted into the lateral ventricle at the coordinates [32]: 0.5 mm posterior to the bregma, 1.0 mm to the right of the central suture, and 2.0 mm deep with the aid of an electrode holder (Stoelting Company, Wood Dale, IL). Cannulas were secured to the skull with orthodontic resin (powder and liquid mixed 1:2, both from Densply International Inc., Milford, DE). After the resin hardened, the scalp wound was closed with silk suture. During recovery, all animals were housed individually with food and water available ad libitum. One week later, mice were tested for learning and other behaviors, levels of Aβ were measured by ELISA, and efflux of I-Aβ_{42} was assessed (as described above).

Brain homogenization and LRP-1 isolation

After a 1 week i.c.v. infusion of either saline, random or antisense cocktail (100 ng/h), the brains were removed, weighed, and homogenized with a polytron bench top homogenizer (Kinematica, Switzerland) at setting 22 in a 5 X volume of extraction buffer A (1 M Tris HCl, 5 M NaCl, 0.5 M EDTA, 0.5 M EGTA, 100 mM Na VO_4, and Protease Inhibitor Cocktail; Sigma) added. Samples were centrifuged (1,000 × g) for 10 min at 4°C, the supernatant removed, centrifuged a second time (21,460 × g for 40 min at 4°C) to separate the cytosolic (supernatant, containing the small subunit of LRP-1) and membrane (pellet) proteins. For all samples, protein levels were quantified with a BCA Protein Assay Kit (Pierce Biotechnology, Rockford, IL).

Western blot for LRP-1

Protein samples from the above samples were separated in either NuPAGE Novex 3–8% Tris-Acetate or NuPAGE Novex 4–12% Bis-Tris precast gels (Invitrogen, Carlsbad, CA). After electrophoresis, protein was transferred onto a nitrocellulose membrane (0.45 μm Pore Size), the membrane washed in Trisbuffered saline (10 mM TrisHcl +150 mM NaCl; pH = 8.0) supplemented with 0.05% Tween 20 (TBS-T), blocked for 1 h at room temperature in a solution of 5% Blotto non-fat dry milk (Santa Cruz Biotechnology) dissolved in TBS-T, and incubated with the primary antibody overnight at 4°C. The following morning, the secondary antibody was diluted in the 5% milk solution and applied to the membrane for 1 h at room temperature. The membrane was washed and a l:l solution of Supersignal West Pico Peroxide Solution and Supersignal West Pico Luminol/Enhancer Solution (Pierce, Rockford, IL) was added. Bands

were visualized by exposure to BioMax XAR Scientific Imaging Film (Kodak) and optical density quantified with Image J analysis software. Antibodies used (Santa Cruz Biotechnology) were the primary anti-LRP-1 antibody for large subunit (rabbit polyclonal IgG, H-80, 1:200), the primary actin antibody (rabbit polyclonal IgG, sc-1616R, 1:5,000), the secondary antibodies (goat anti-rabbit) IgG conjugated to horseradish peroxidase (HRP), sc-2004, 1:10,000), and a goat anti-mouse IgG conjugated to HRP (sc-2005; 1:10,000). The primary anti-LRP-1 antibody for the small 85 kDa subunit was a mouse monoclonal IgG (Calbiochem, 5A6, 1:1,000).

Aβ extraction from brain

Total Aβ was extracted from hemibrains by placing them in cold extraction buffer (50 mM NaCl, 0.2% diethylamine (DEA) and adding 1x Protease Inhibitor Cocktail, Sigma) at a concentration of 1 mL buffer/200 mg tissue. Samples were homogenized (PowerMax AHS 200, VWR) and centrifuged at 100,000 × g for 30 min. The supernatant was removed and a 10% volume of neutralization buffer (1.0 M Tris-HCl, pH = 6.2) added prior to storage at −80° C.

Aβ ELISA

Details of two-site sandwich ELISA procedures and antibodies for rodent Aβ have been published [33–35]. Carboxy-terminal specific antibody 13.1.1 was used for the detection of Aβ_{40}, and 2.1.3 was used for Aβ_{42}; rodent specific amino-terminal antibody (32.4.1) was used for both forms. Capture antibody was added (1.0 μg/well, in standard PBS, pH = 7.4) to each of the inner wells of an Immunolon 96-well HBX Plate. Plates were blocked with blocking buffer [PBS, 1% Block Ace™ (Serotec), 1% BSA, 0.05% NaN_3, pH = 7.4]. Next, 50 μL of AC buffer [0.02 M sodium phosphate buffer (pH = 7), 0.4 M NaCl, mM EDTA, 0.4% Block Ace™, 0.2% BSA, 0.05% CHAPS, and 0.05% NaN_3] was added to prevent wells from drying while loading. Synthetic peptide standards (Chemicon) were prepared in neutralized extraction buffer. Standards and samples were loaded at least in duplicate at a quantity of 100 μL per well. After overnight capture at 4°C, plates were washed extensively with PBST (PBS + 0.05% Tween-20) and 100 ng/well of HRP-conjugated antibody 13.1.1, in buffer D [0.02 M sodium phosphate, 0.0002% thimerosal, 2 mM EDTA, 0.4 M NaCl and 1% BSA, pH = 7.0], was added to each well. After a second overnight incubation, plates were again washed extensively with PBST, and developed with TMB reagent (Kirkegaard & Perry Laboratories). The reaction was stopped with 6% o-phosphoric acid and read at 450 nm using a BioTek multiwell plate reader.

Active avoidance T-maze

This behavioral test as described previously [36,37] was used to assess spatial learning in cocktail, random antisense and saline treated animals. The T-maze apparatus was a black, plastic alley (46 cm long) with a start box at one end and two goal boxes (17.5 cm long) at the opposite end. The maze had a depth of 12.5 cm and a width of 9.8 cm throughout. The floor of the maze consisted of stainless steel rods. The start box of the maze was separated from the alley by a plastic guillotine door that prevented the mouse from entering the alley before the training started.

A training trial began by placing a mouse into the start box and raising the guillotine door while sounding a 65 db warning buzzer (conditioned stimulus). After 5 s in the maze, 0.35 mA of footshock (unconditioned stimulus) was applied from a Coulbourn Instruments scrambled grid floor shocker (model E 13-08). The first goal box the mouse entered on the first trial was designated as the incorrect choice. At the end of each trial, the mouse was removed from the goal box and returned to its home cage. After a 45 s intertrial interval, a new trial began. The mouse received footshock if it remained in the start compartment or entered the incorrect goal box, whereas entry into the correct goal box terminated the buzzer and footshock. Training

continued until the mouse learned to enter the correct goal box in less than 5 s, thereby avoiding footshock. All mice were trained until they made their first avoidance of footshock. Acquisition test scores were expressed as the mean trials until first footshock avoidance was made.

Open field (Locomotor) activity

Mice were tested in a circular open field arena 45 cm in diameter with clear plexiglass sides that were'30 cm high. Mice were given one 15 min trial to freely explore the open field. A testing session began when the mouse was placed on one side of in the arena and facing the wall. The distance each mouse traveled during the session was recorded in centimeters using a Polytrak recording system (San Diego Instruments, San Diego, CA). The mean distance traveled for each treatment group was expressed as the percent of the control group.

Recognition of a novel object

This method has been described previously [37]. Prior to testing, mice were habituated for three consecutive days to the testing apparatus (a 58 × 66 × 11 cm white, plastic box). During habituation, each mouse was allowed to freely explore the testing apparatus for 5 min. On the first day of training, mice were placed in the testing apparatus for 5 min and allowed to explore a pair of identical objects (objects A and B; both were 7 × 6.3 × 5.1 cm). On the second day of training, one of the original objects was replaced with a new, or novel object (Object C; 8.2 × 3.8 × 7.4 cm). Mice were placed in the testing apparatus for 5 min and the amount of time each mouse spent sniffing or touching of the novel object was recorded. Results were expressed as the percent of time spent investigating the novel object.

Statistics

Statistical differences between two groups were determined using Student's t-test with Dunnets post test. In experiments with more than two means, a one-way or a two-way analysis of variance (ANOVA) was used followed by Newman-Keuls or Bonferroni multiple comparison post-test, respectively. All statistical analyses were carried out using GraphPad, Prism Software (GraphPad, San Diego, CA).

RESULTS

Effect of cocktail on LRP-1 expression in isolated MBMs

Immunohistochemistry was used to verify that the cocktail could reduce LRP-1 protein expression *in vitro* in brain microvasculature. For this study, we used isolated MBMs which, unlike cultured BMECs, do not dedifferentiate [38].

Figure 1 shows phase contrast (a,c,e) and immunofluorescence (b,d,f) micrographs of isolated MBMs that were treated with either incubation buffer, random antisense, or antisense cocktail (10 μg/mL) for 24 h. Treatment with cocktail was associated with decreased immunofluorescence, indicating reduced LRP-1. Figure 1g shows the mean fluorescent intensity for each treatment group. Analysis by one-way ANOVA revealed that MBMs treated with cocktail demonstrated significantly less ($F_{2,11} = 6.20$, $p < 0.05$) fluorescent intensity (66.5%) compared to buffer and random antisense treated MBMs (100% and 111.14%, respectively).

Effects of cocktail on I-Aβ_{42} efflux in BMEC cultures

We then tested the effectiveness of the cocktail in primary mouse BMEC cultures, an *in vitro* model of the BBB. As this model can become undifferentiated from the BBB phenotype, we first verified the presence of LRP-1. Results in figure 1h show that 1 μg/mL of Aβ_{42} added to the abluminal chamber of the Transwell insert significantly ($p < 0.01$) inhibited abluminal-

to-luminal transport of Aβ that had been radioactively labeled with I^{131} (I-Aβ_{42}). This demonstrates the presence of a saturable efflux transporter for I-Aβ_{42} in the BMEC cultures.

In Fig. 1i, BMEC cultures were treated with either random or cocktail antisense for 24 h at a concentration of either 1 μg/mL or 10 μg/mL. A two-way analysis of variance (ANOVA) showed that treatment with the cocktail had a significant effect ($F_{1,46} = 8.92$, $p < 0.01$) on I-Aβ_{42} efflux ($p < 0.05$) with no difference between the doses. These results show that treatment with the cocktail can produce a functional decrease in I-Aβ_{42} efflux *in vitro*.

CNS pharmacokinetics of i.v. cocktail PS-ODNs

We then wanted to determine whether the 19mer and 23mer were effective *in vivo*. We first tested whether they were taken up by the brain and BBB after i.v. injection and whether they could affect LRP-1 activity at the BBB. After injection into the jugular vein, significant brain uptake was found for both P-19mer (Fig. 2a, Ki = 0.18 ± 0.02 μl/g-min) and P-23mer (Fig. 2b, Ki = 0.20 ± 0.01 μl/g-min). Co-administration of unlabeled PS-ODN significantly reduced uptake of the P-23mer (Fig. 2d), but not the P-19mer (Fig. 2c). Capillary depletion with vascular washout showed that most of the PS-ODNs crossed the BBB [29] to be taken up by brain tissue (Fig. 2e–f). Some material was also sequestered by the brain capillaries and since the capillaries on a weight basis are about 1/100 that of the brain parenchyma, the concentration the PS-ODNs would have been very high in the capillary fraction. A one-way ANOVA of mean regional uptake for the P-19mer (Fig. 2g) and P-23mer (Fig. 2h) showed that, for both PS-ODNs, there were significant regional differences in brain uptake ($F_{2,56} = 1190$, $p < 0.001$ and $F = F_{2,56} = 18080$, $p < 0.0001$ respectively) with the highest uptake into the hippocampus.

Functional effect of i.v. cocktail on brain efflux of I-Aβ$_{42}$

Figure 3a shows mice that were treated with i.v. (tail vein) cocktail or saline and, at various times afterwards, were then give I-Aβ_{42} by i.c.v. injection to determine brain efflux. Results showed that 12 h after i.v. cocktail there was a significant decrease in I-Aβ_{42} efflux compared to saline treated mice ($p < 0.001$). This roughly corresponds with the half-life of LRP-1 in human glioblastoma cells, reported as about 8–10 h [39]. A rebound in efflux activity occurred 24 h after a single injection of i.v. cocktail. Mice treated with a second i.v. dose of cocktail 12 h after the first and studied another 12 h later (24 h after the first injection of cocktail) showed near total inhibition of I-Aβ_{42} efflux activity (Fig. 3a, right Y axis). We also injected the I-Aβ_{42} directly into the hippocampus in mice treated with cocktail or saline 12 h previously (Fig. 3b). Efflux ofI-Aβ_{42} from hippocampal tissue into the blood was decreased by over 50% [$t(24) = 3.09$, $p < 0.01$].

Figure 3c shows that the two-injection regimen used in Fig. 3a produced a significant decrease in brain mRNA for LRP-1 for cocktail but not for random antisense ($F_{2,6} = 6.61$, $p < 0.05$). Neither LRP-antisense cocktail nor the random antisense had any effect on mRNA for the receptor for advanced glycated end products (RAGE), which is the blood-to-brain transporter for Aβ.

RAP is also a ligand for LRP-1. Figure 3e shows that RAP inhibits the brain-to-blood efflux of i.c.v. administered I-Aβ_{42} [$t(16) = 5.42$, $p < 0.001$], confirming that RAP is a competitive ligand for Aβ at the BBB. We then confirmed that our cocktail to LRP-1 also inhibited brain-to-blood efflux of radioactively labeled RAP: $t(24) = 4.47$, $p < 0.01$. Thus, we showed that the antisense cocktail specifically inhibited efflux of two of the major ligands of LRP-1: RAP and Aβ.

Pharmacokinetics of i.v. cocktail PS-ODNs for the liver

We then compared the relative uptake of P-19mer and P-23mer by brain and liver, another tissue that expresses high levels of LRP-1. Table 1 compares the percent of the i.v. injected dose taken up per gram of brain or liver for each of the cocktail PS-ODNs 2–30 min after their i.v. injection. Table I shows that about 100 times more PS-ODN was taken up by liver than by brain.

CNS pharmacokinetics and effects of i.c.v. PS-ODNs

We then explored i.c.v. infusion of antisense cocktail as a more targeted approach for delivery of the brain. Figure 4a (P-19mer) and 4b (P23mer) shows that after i.c.v. injection, these two antisenses tended to be retained by brain, with half-time clearances 231.5 min and 47.8 min, respectively. Such retention allowed us to give lower doses of antisense with little concern that the antisense would enter the circulation in significant amounts.

Figure 4c shows the effects of i.c.v. cocktail (200 ng) on I-Aβ_{42} brain efflux. Mice were treated with i.c.v. cocktail or saline and, either 30 min or 24 h later, administered i.c.v. I-Aβ_{42}. At t = 30 min, there was no affect on I-Aβ_{42} efflux. At 24 h, however, cocktail treated mice had significantly decreased brain efflux of I-Aβ_{42} ($F_{2.38} = 10.32$, $p < 0.001$). The transport of two other peptides previously shown to be effluxed from the brain by other transport systems, the 27 amino acid form of the pituitary adenylate cyclase activating peptide (PACAP-27) and melanocyte stimulating hormone inhibitory factor 1 (Tyr-MIF-1) were not affected 24 h after treatment with cocktail (data not shown).

Figure 4d compares efflux of I-Aβ_{42} in mice treated with the cocktail, random antisense, or an antisense to AβPP known to decrease Aβ levels in brain. Statistical differences were found ($F_{3,63} = 31.7$, $p < 0.0001$) with the post-test showing that cocktail decreased efflux of I-Aβ_{42} ($p < 0.01$). In contrast, the antisense to AβPP increased the efflux rate of I-Aβ_{42} ($p < 0.01$), consistent with a decreased level of endogenous ligand.

Effects of chronic i.c.v. cocktail on brain efflux of I-Aβ$_{42}$, *brain levels of endogenous mouse Aβ, and behavior*

In these studies, mice were infused chronically with i.c.v. cocktail for 1 week (100 ng/h) to produce a sustained decrease in LRP-1 expression. Figure 5a shows typical Western blots for the 85kDa subunit of LPR-1 and actin in saline (S), random antisense (R), and cocktail (C) treated mice and Fig. 5b the quantitation ($p < 0.05$). Figure 5c shows I-Aβ_{42} efflux in mice treated with saline, random and cocktail antisense. Results show that mice infused with cocktail demonstrate significantly less I-Aβ_{42} efflux when compared to saline ($p < 0.001$) and random ($p < 0.01$) antisense treated mice ($F_{2,39} = 14.90$, $p < 0.001$).

To determine whether the i.c.v. cocktail infusion (1 wk; 100 ng/h) altered brain levels of endogenous mouse Aβ, we used an ELISA to quantify brain levels of either Aβ_{40} (Fig. 5d) or Aβ_{42} (Fig. 5e). Results showed that cocktail-treated mice had significantly higher levels of Aβ_{42} compared to both saline ($p < 0.05$) and random ($p < 0.01$) treated mice ($F_{2,13} = 7.97$, $p < 0.01$). Although brain levels of Aβ_{40}, showed a similar trend, the results did not reach statistical significance ($0.05 < p < 0.10$).

We then tested mice for impaired learning and memory. We tested for hippocampal-mediated spatial learning in an auditory-cued, active avoidance T-Maze. Cocktail treated mice exhibited a higher mean acquisition score (Fig. 5f) than either the saline and random antisense treated mice ($F_{2,39} = 7.163$, $p < 0.01$), showing that cocktail treated mice required significantly more trials in the maze to learn to avoid footshock. These mice showed no decrease in locomotor

activity as measured in the open field test (Fig. 5g), ruling out this as a confounder for the T-maze test.

Cocktail and random treated mice (2 wk i.c.v. infusion; 100 ng/h) were also assessed for recognition memory in the novel object recognition task (Fig. 5f). Mice showed no differences in total exploration time (data not shown). However, mice treated with the random antisense spent a majority of their time investigating the new object, indicating memory of the original object. Cocktail treated mice, however, spent significantly [$t(26) = 2.12$), $p < 0.05$] less time investigating the novel object. This indicates that treatment with the cocktail was associated with impairment in recognition memory for the previously explored object.

DISCUSSION

According to the neurovascular hypothesis, impaired clearance of Aβ by LRP-1 at the BBB leads to increased Aβ accumulation in brain and progression of AD [10]. Aβ is transported across the BBB in both the blood-to-brain and brain-to-blood directions by RAGE and LRP-1, respectively [40–43]. Decreased clearance from brain would lead to unopposed influx of Aβ across the BBB and increased retention by brain of Aβ. Increased retention and influx of Aβ has been associated with numerous mechanisms related to AD-associated pathologies, including inflammation [44] and oxidative stress [45]. Previous research has shown that LRP-1 is involved in efflux of Aβ from the brain [13,46]. Until now, it has not been possible to directly test the neurovascular hypothesis because deletion of the gene that encodes for LRP-1 produces embryonic lethality in mice [15]. Here, we have designed an antisense cocktail directed at LRP-1 so that we could conduct a test of the neurovascular hypothesis *in vivo*. Before administering our cocktail to mice, we first tested it for efficacy in two different *in vitro* models of the BBB. In these models, we found that our antisenses decreased LRP-1 protein expression in brain endothelial cells and the abluminal-to-luminal efflux of Aβ.

We next examined the effects of our cocktail *in vivo* and found that both the P-19mer and P-23mer were taken up by the BBB, whole brain, and hippocampus where it selectively decreased LRP-1 mRNA and inhibited brain-to-blood efflux of two LRP-1 ligands: Aβ and RAP. This is consistent with the BBB uptake and transport of other PS-ODNs [20]. Although these results supported our ability to test the neurovascular hypothesis with our antisenses, we noted that i.v. administration also resulted in uptake by the liver some 100 times greater than by brain. This raised the possibility that liver LRP-1 might be affected which would have unknown effects on cognition. We, therefore, opted to test the effect of our antisenses on cognition after direct injection into the brain.

We first tested the retention of i.c.v. administered antisense and its effects on Aβ efflux. We found that very little efflux into blood of the PS-ODNs occurred after i.c.v. administration and that a dose of about 1/70 of the i.v. dose was effective at inhibiting Aβ efflux. We also found that a single i.c.v. injection of the cocktail produced a decrease in I-Aβ_{42} efflux 24 h after administration, whereas mice treated with a single i.v. injection of cocktail showed rebound of efflux activity by 24 h. Previous pharmacokinetic studies conducted on PS-ODNs have shown that, regardless of route of administration, these analogs can be recovered from the central nervous system (CNS) intact for several hours after delivery [18,19]. Such long activity once inside the brain may be because the antisense is no longer exposed to serum nucleases and therefore will not be degraded as rapidly.

To produce the more prolonged decrease in LRP-1 expression needed for behavioral testing, we delivered our cocktail chronically by i.c.v. infusion. We found that all the predictions of the neurovascular hypothesis were met in mice treated with i.c.v. antisense for one week. The antisense cocktail, but not random antisense, decreased LRP-1 protein levels by about 50%

and produced a similar decrease in the brain-to-blood efflux rate of Aβ. Levels of immunoactive Aβ, especially of Aβ_{42}, increased in brain by about 30%. Impairment in learning was found in the hippocampal-dependent T-maze and impairment in memory was found in the hippocampal-dependent novel object recognition task.

In conclusion, our results show that a defect in LRP expression leads to impaired clearance of Aβ from the brain, an accumulation in brain of Aβ, and impaired cognition. These results, therefore, strongly support the neurovascular hypothesis as a mechanism in the progression of AD. Restoration of the ability of the BBB to effectively remove Aβ from brain or prevention of the development of impaired LRP function at the BBB are possible therapeutic strategies in the treatment of AD.

Acknowledgments

Supported by VA Merit Review, R01 NS050547, and AG029839.

REFERENCES

[1]. Hebert LE, Scherr PA, Bienias JL, Bennett DA, Evans DA. Alzheimer disease in the US population; prevalence estimates using the 2000 census. Arch Neurol 2003;60:1119–1122. [PubMed: 12925369]

[2]. Selkoe DJ. The cell biology of the β-amyloid precursor protein and presenilin in Alzheimer's disease. Trends Cell Biol 1998;8:447–453. [PubMed: 9854312]

[3]. Selkoe DJ. Normal and abnormal biology of the β-amyloid precursor protein. Rev Neurosci 1994;17:489–517.

[4]. Gravina SA, Ho L, Eckman CB, Long KE, Otvos L Jr. Younkin LH, Suzuki N, Younkin SG. Amyloid beta protein (A beta) in Alzheimer's disease brain. Biochemical and immunocytochemical analysis with antibodies specific for forms ending at A beta 40 or A beta 42(43). J Biol Chem 1995;270:7013–7016. [PubMed: 7706234]

[5]. Iwatsubo T, Odaka A, Suzuki N, Mizusawa H, Nukina N, Ihara Y. Visualization of A beta 42(43) and A beta 40 in senile plaques with end-specific A beta monoclonals: evidence that an initially deposited species is A beta 42(43). Neuron 1994;13:45–53. [PubMed: 8043280]

[6]. Jaeger LB, Banks WA. Antisense therapeutics and the treatment of CNS disease. Front Biosci 2004;9:1720–1727. [PubMed: 14977581]

[7]. Masters CL, Simms G, Weinman NA, Multhaup G, McDonald BL, Beyreuther K. Amyloid plaque core protein in Alzheimer disease and Down syndrome. Proc Natl Acad Sci USA 1985;82:4245–4249. [PubMed: 3159021]

[8]. Hock BJ Jr. Lamb BT. Transgenic mouse models of Alzheimer's disease. Trends Genet 2001;17:S7–S12. [PubMed: 11585670]

[9]. Eckman EA, Watson M, Marlow L, Sambamurti K, Eckman CB. Alzheimer's disease beta-amyloid peptide is increased in mice deficient in endothelin-converting enzyme. J Biol Chem 2003;278:2081–2084. [PubMed: 12464614]

[10]. Zlokovic BV. Neurovascular mechanisms of Alzheimer's neurodegeneration. Trends Neurosci 2005;28:202–208. [PubMed: 15808355]

[11]. Deane R, Sagare A, Zlokovic B. The role of the cell surface LRP and soluble LRP in blood-brain barrier Aβ clearance in Alzheimer's disease. Curr Pharm Design 2008;14:1601–1605.

[12]. Zlokovic BV. Cerebrovascular transport of Alzheimer's amyloid beta and apolipoproteins J and E: possible anti-amyloidogenic role of the blood-brain barrier. Life Sci 1996;59:1483–1497. [PubMed: 8890929]

[13]. Shibata M, Yamada S, Kumar SR, Calero M, Bading J, Frangione B, Holtzman DM, Miller CA, Strickland DK, Ghiso J, Zlokovic BV. Clearance of Alzheimer's amyloid-β 1-40 peptide from brain by LDL receptor-related protein-1 at the blood-brain barrier. J. Clin Invest 2000;106:1489–1499. [PubMed: 11120756]

[14]. Kang DE, Pietrzik CU, Baum L, Chevallier N, Merriam DE, Kounnas MZ, Wagner SL, Troncoso JC, Kawas CH, Katzman R, Koo EH. Modulation of amyloid beta-protein clearance and Alzheimer's disease susceptibility by the LRL receptor-related protein pathway. J. Clin Invest 1998;106:1159–1166. [PubMed: 11067868]

[15]. Willnow T, Armstrong S, Hammer R, Herz J. Functional expression of low density lipoprotein receptor-related protein is controlled by receptor-associated protein *in vivo*. Proc Natl Acad Sci USA 1995;92:4537–4541. [PubMed: 7538675]

[16]. Banks WA, Robinson SM, Verma S, Morley JE. Efflux of human and mouse amyloid beta proteins 1-40 and 1-42 from brain: impairments in a mouse model of Alzheimer's disease. Neuroscience 2003;121:487–492. [PubMed: 14522007]

[17]. Jaeger, LB.; Banks, WA. Transport of antisense across the blood-brain barrier. In: Phillips, MI., editor. Methods Mol Med: Antisense Therapeutics. Humana Press Inc.; New Jersey: 2005. p. 237-251.

[18]. Banks WA, Farr SA, Butt W, Kumar VB, Franko MW, Morley JE. Delivery across the blood-brain barrier of antisense directed against amyloid β: reversal of learning and memory deficits in mice overexpressing amyloid precursor protein. J Pharmacol Exp Ther 2001;297:1113–1121. [PubMed: 11356936]

[19]. Dogrukol-Ak D, Kumar VB, Ryerse JS, Farr SA, Verma S, Nonaka K, Nakamachi T, Ohtaki H, Niehoff ML, Edwards JC, Shioda S, Morley JE, Banks WA. Isolation of peptide transport system-6 from brain endothelial cells: therapeutic effects with antisense inhibition in Alzheimer's and stroke models. J. Cereb Blood Flow Metab 2009;29:411–422. [PubMed: 19002200]

[20]. Banks WA, Jaeger LB, Urayama A, Kumar VB, Hileman SM, Gaskin FS, Llanza NV, Farr SA, Morley JE. Preproenkephalin targeted antisenses cross the blood-brain barrier to reduce brain methionine enkephalin levels and increase voluntary ethanol drinking. Peptides 2006;27:784–796. [PubMed: 16229925]

[21]. Mare S, Penugonda S, Robinson SM, Dohgu S, Banks WA, Ercal N. Copper complexing decreases the ability of amyloid beta peptide to cross the BBB and enter brain parenchyma. Peptides 2004;43:333–344.

[22]. Szabó CA, Deli MA, Ngo TKD, Joó F. Production of pure primary rat cerebral endothelial cell culture: a comparison of different methods. Neurobiology 1997;5:1–16. [PubMed: 9302692]

[23]. Perriére N, Demeuse P, Garcia E, Regina A, Debray M, Andreux JP, Couvreur P, Scherrmann JM, Temsamani J, Couraud PO, Deli MA, Roux F. Puromycin-based purification of rat brain capillary endothelial cell cultures. Effect on the expression of blood-brain barrier-specific properties. J Neurochem 2005;93:279–289. [PubMed: 15816851]

[24]. Dehouck MP, Jolliet-Riant P, Brée F, Fruchart JC, Cecchelli R, Tillement JP. Drug transfer across the blood-brain barrier: correlation between *in vitro* and *in vivo* models. J Neurochem 1992;58:1790–1797. [PubMed: 1560234]

[25]. Gerhart DZ, Broderius MA, Drewes LR. Cultured human and canine endothelial cells from brain microvessels. Brain Res Bull 1998;21:785–793. [PubMed: 3219610]

[26]. Blasberg RG, Fenstermacher JD, Patlak CS. Transport of alpha-aminoisobutyric acid across brain capillary and cellular membranes. J. Cereb Blood Flow Metab 1983;3:8–32. [PubMed: 6822623]

[27]. Morley JE, Farr SA, Flood JF. Antibody to amyloid beta protein alleviates impaired acquisition, retention, and memory processing in SAMP8 mice. Neurobiol Learn Mem 2002;78:125–138. [PubMed: 12071671]

[28]. Banks WA, Coon AB, Robinson SM, Moinuddin A, Shultz JM, Nakaoke R, Morley JE. Triglycerides induce leptin resistance at the blood-brain barrier. Diabetes 2004;53:1253–1260. [PubMed: 15111494]

[29]. Triguero D, Buciak J, Pardridge WM. Capillary depletion method for quantification of blood-brain barrier transport of circulating peptides and plasma proteins. J. Neurochem 1990;54:1882–1888. [PubMed: 2338547]

[30]. Gutierrez EG, Banks WA, Kastin AJ. Murine tumor necrosis factor alpha is transported from blood to brain in the mouse. J Neuroimmunol 1993;47:169–176. [PubMed: 8370768]

[31]. Jaeger LB, Banks WA, Varga JL, Schally AV. Antagonists of growth hormone-releasing hormone cross the blood-brain barrier: A potential applicability to treatment of brain tumors. Proc Natl Acad Sci USA 2005;102:12495–12500. [PubMed: 16118272]

[32]. Slotnick, BM.; Leonard, CM. A stereotaxic atlas of the albino mouse forebrain. U.S. Department of Health; Washington DC: 1975.

[33]. Ramsden M, Nyborg AC, Murphy MP, Chang L, Stanczyk FZ, Golde TE, Pike CJ. Androgens modulate beta-amyloid levels in male rat brain. J. Neurochem 2003;87:1052–1055. [PubMed: 14622134]

[34]. Das P, Howard V, Loosbrock N, Dickson D, Murphy MP, Golde TE. Amyloid-beta immunization effectively reduces amyloid deposition in FcRgamma−/− knock-out mice. J Neurosci 2003;23:8532–8538. [PubMed: 13679422]

[35]. Kukar T, Murphy MP, Eriksen JL, Sagi SA, Weggen S, Smith TE, Ladd T, Khan MA, Kache R, Beard J, Dodson M, Merit S, Ozols VV, Anastasiadis PZ, Das P, Fauq A, Koo EH, Golde TE. Diverse compounds mimic Alzheimer disease-causing mutations by augmenting Abeta42 production. Nat Med 2005;11:545–550. [PubMed: 15834426]

[36]. Diano S, Farr SA, Benoit SC, McNay EC, da Silva I, Horvath B, Gaskin FS, Nonaka N, Jaeger LB, Banks WA, Morley JE, Pinto S, Sherwin RS, Xu L, Yamada KA, Sleeman MW, Tschöp M, Horvath TL. Ghrelin controls hippocampal spine synapse density and memory performance. Nat Neurosci 2006;9:381–388. [PubMed: 16491079]

[37]. Jaeger LB, Farr SA, Banks WA, Morley JE. Effects of orexin-A on memory processing. Peptides 2002;23:1683–1688. [PubMed: 12217429]

[38]. Joo F. The blood-brain barrier *in vitro*: the second decade. Neurochem Int 1993;23:499–521. [PubMed: 8281119]

[39]. Bu G, Maksymovitch EA, Gueze H, Schwartz AL. Subcellular localization and endocytic function of low density lipoprotein receptor-related protein in human glioblastoma cells. J Biol Chem 1994;47:29874–29882. [PubMed: 7961982]

[40]. Deane R, Yan SD, Submamaryan RK, LaRue B, Jovanovic S, Hogg E, Welch D, Manness L, Lin C, Yu J, Zhu H, Ghiso J, Frangione B, Stern A, Schmidt AM, Armstrong DL, Arnold B, Liliensiek B, Nawroth P, Hofman F, Kindy M, Stern D, Zlokovic B. RAGE mediates amyloid-β peptide transport across the blood-brain barrier and accumulation in brain. Nat Med 2003;7:907–913. [PubMed: 12808450]

[41]. Maness LM, Banks WA, Podlisny MB, Selkoe DJ, Kastin AJ. Passage of human amyloid β protein 1-40 across the murine blood-brain barrier. Life Sci 1994;21:1643–1650. [PubMed: 7968239]

[42]. Pan W, Solomon B, Maness LM, Kastin AJ. Antibodies to ß-amyloid decrease the blood-to-brain transfer of ß-amyloid peptide. Exp Biol Med 2002;227:609–615.

[43]. Ghersi-Egea JF, Gorevic PD, Ghiso J, Frangione B, Patlak CS, Fenstermacher JD. Fate of cerebrospinal fluid-borne amyloid β-peptide: rapid clearance into blood and appreciable accumulation by cerebral arteries. J Neurochem 1996;67:880–883. [PubMed: 8764620]

[44]. Giri R, Shen Y, Stins M, Du Yan S, Schmidt AM, Stem D, Kim KS, Zlokovic B, Karla VK. Beta-amyloid-induced migration of monocytes across human brain endothelial cells involves RAGE and PECAM-1. Am J Physiology 2000;279:C1772–C1781.

[45]. Poon HF, Farr SA, Banks WA, Pierce WM, Klein JB, Morley JE, Butterfield DA. Proteomic identification of less oxidized brain proteins in aged senescence-accelerated mice following administration of antisense oligonucleotide directed at the Abeta region of amyloid precursor protein. Mol Brain Res 2005;138:8–13. [PubMed: 15932783]

[46]. Deane R, Wu Z, Sagare A, Davis J, Du Yan S, Hamm K, Xu F, Parisi M, LaRue B, Hu HW, Spijkers P, Guo H, Song X, Lenting PJ, Van Nostrand WE, Zlokovic BV. LRP/amyloid beta-peptide interaction mediates differential brain efflux of Abeta isoforms. Neuron 2004;43:333–344. [PubMed: 15294142]

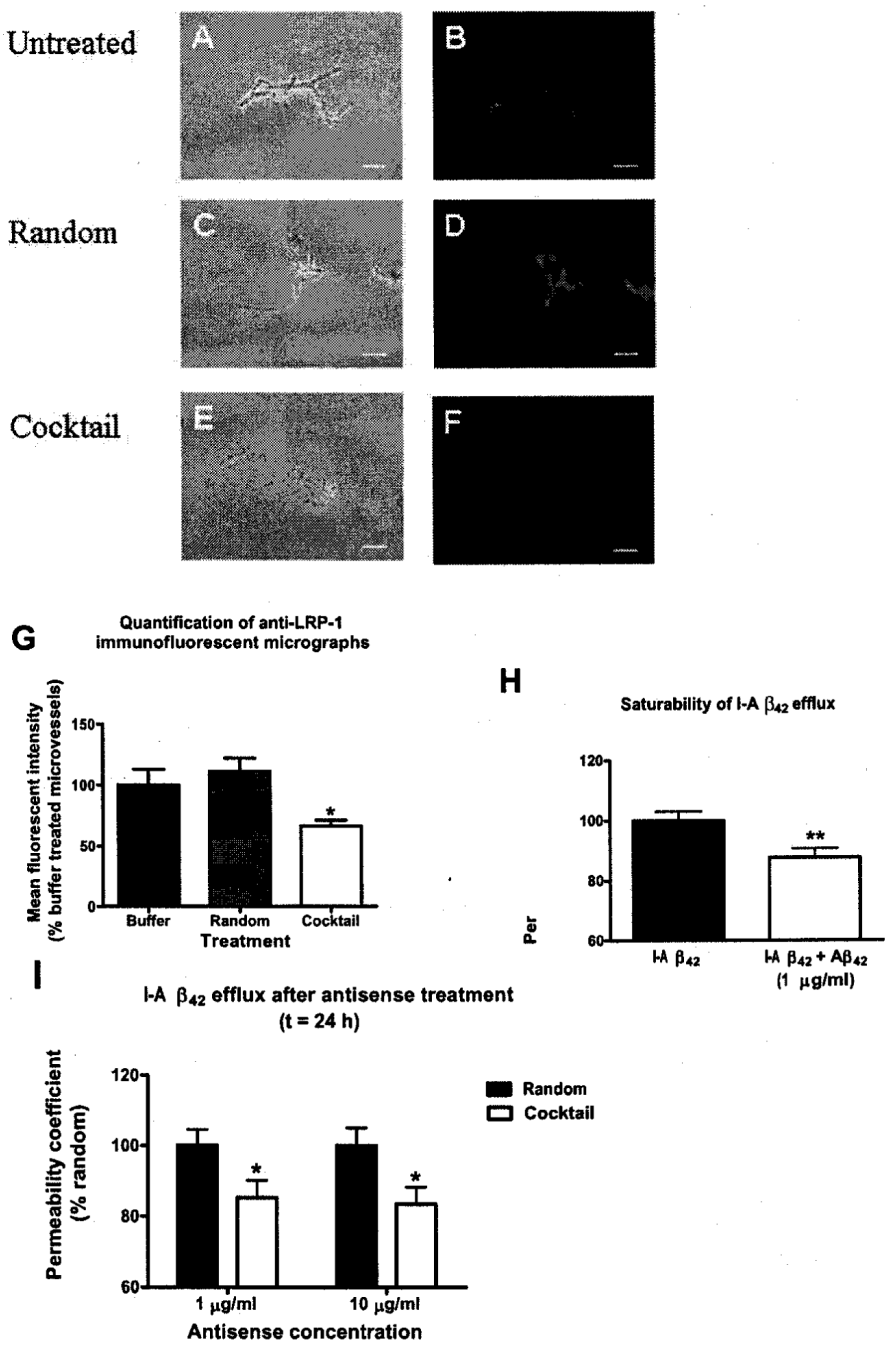

Fig. 1.

Effects of antisense cocktail treatment *in vitro*: BMEC monolayers and isolated mouse brain microvessels (MBMs). (**A-G**) Effect of antisense cocktail on LRP-1 expression in isolated MBMs. Representative phase contrast (a, c, and e) and immunofluorescent)b, d, and f) micrographs of MBMs after 24 h treatment with 1 mL incubation buffer (a–b), random antisense (c–d) or antisense cocktail (10 μg/mL) (e–f). Bar = 50 μm. Quantification of immunofluorescent micrographs (g) shows that cocktail treated MBMs exhibit significantly less mean fluorescent intensity than MBMs treated with random antisense or incubation buffer (n = 5-6 slides/group). (**H**) Saturability of I-Aβ_{42} transport in primary BMEC monolayers. Addition of 1 μg of unlabeled Aβ_{42} significantly impaired abluminal to luminal efflux of I-

Aβ_{42}. (**I**) Effects of antisense cocktail treatment on primary BMEC monolayers. Treatment with antisense cocktail (at a dose of 1 μg/ml or 10 μg/ml) significantly impaired efflux of I-Aβ_{42} (n = 13–15/group for h, n = 8–17/group for i). Data shown as mean +/− SEM *p < 0.05; * *p < 0.01. (Colours are visible in the electronic version of the article at www.iospress.nl)

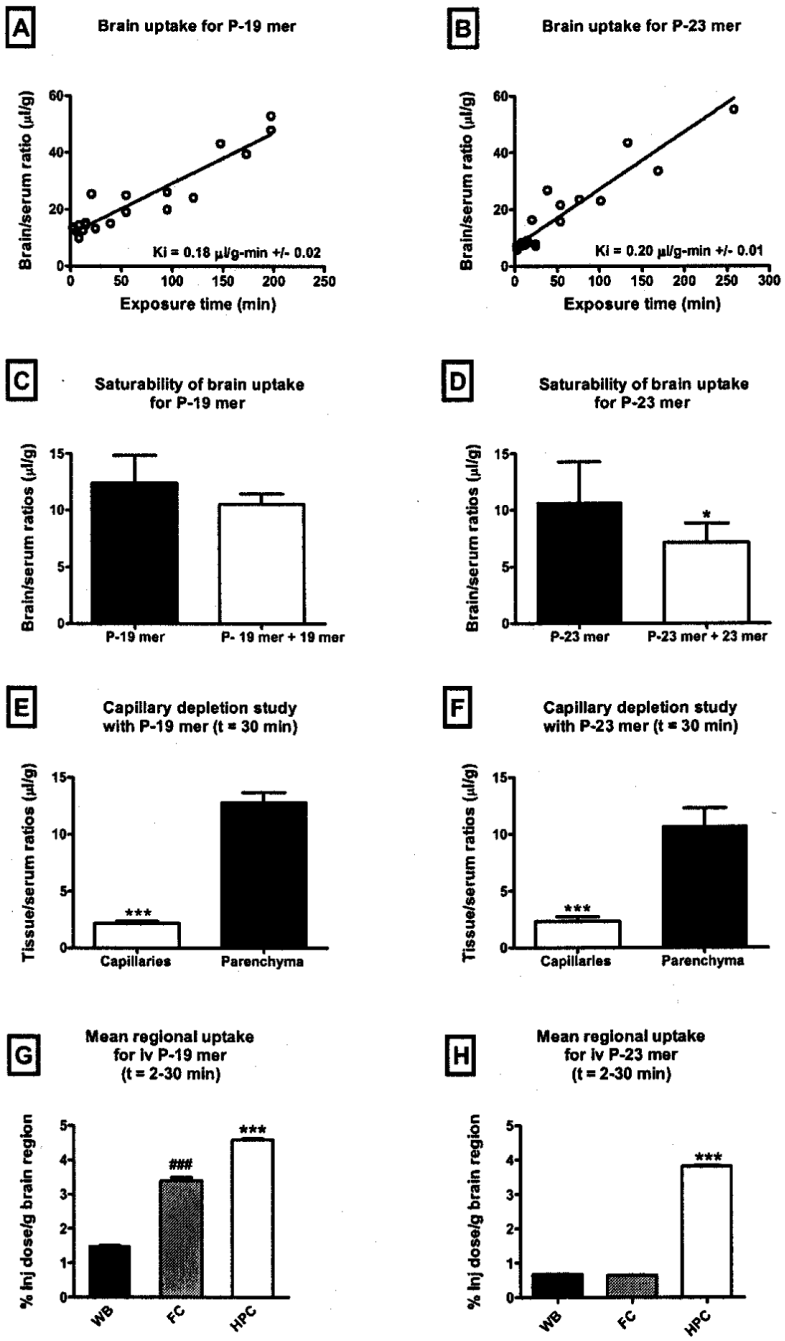

Fig. 2.

CNS pharmacokinetics of i.v. cocktail PS-ODNS *in vivo*. (**A-B**) Brain uptake of i.v. P-19mer and (b) P-23mer cocktail PS-ODNs. The linear relationship between the brain/serum ratios and their relative exposure times (Expt) represents the rate of brain influx (Ki) which is 0.18 μl/g-min +/− 0.02 for the P-19mer (n = 22) and 0.20 μl/g-min +/− 0.01 for the P-23mer (n = 19). (**C-D**) Saturability of brain uptake for P-19mer (c) and P-23mer (d) cocktail PS-ODNs. Co-administration of 10 μg of unlabeled 23mer antisense significantly decreased uptake of P-23 mer. Uptake of P=19mer, however, was not significantly decreased. * = $p < 0.05$. Data shown as mean +/− s.d. (n = 8−9/group). (**E-F**) Distribution of i.v. P-19mer (e) and P-23mer (f) cocktail PS-ODNs between capillary and parenchymal tissues. Both P-Olgs, demonstrated considerable

uptake into the target, the brain capillaries. * * * = $p < 0.001$. (n = 4–9/tissue). (**G-H**) Regional distribution of i.v. P-19mer (**G**) and P-23mer (**H**) in the frontal cortex (FC) and hippocampus (HPC). For the P-23mer, mean uptake into the HPC was significanlty greater than mean uptake into FC and whole brain (WB). Uptake of the P-19mer in the HPC was greater than the uptake into the WB, however, it was not significantly different than the uptake per gram of FC. Data shown as mean +/− SEM (n = 14-23/brain region). ***$p < 0.001$ vs FC and WB; ***$p < 0.001$ vs WB.

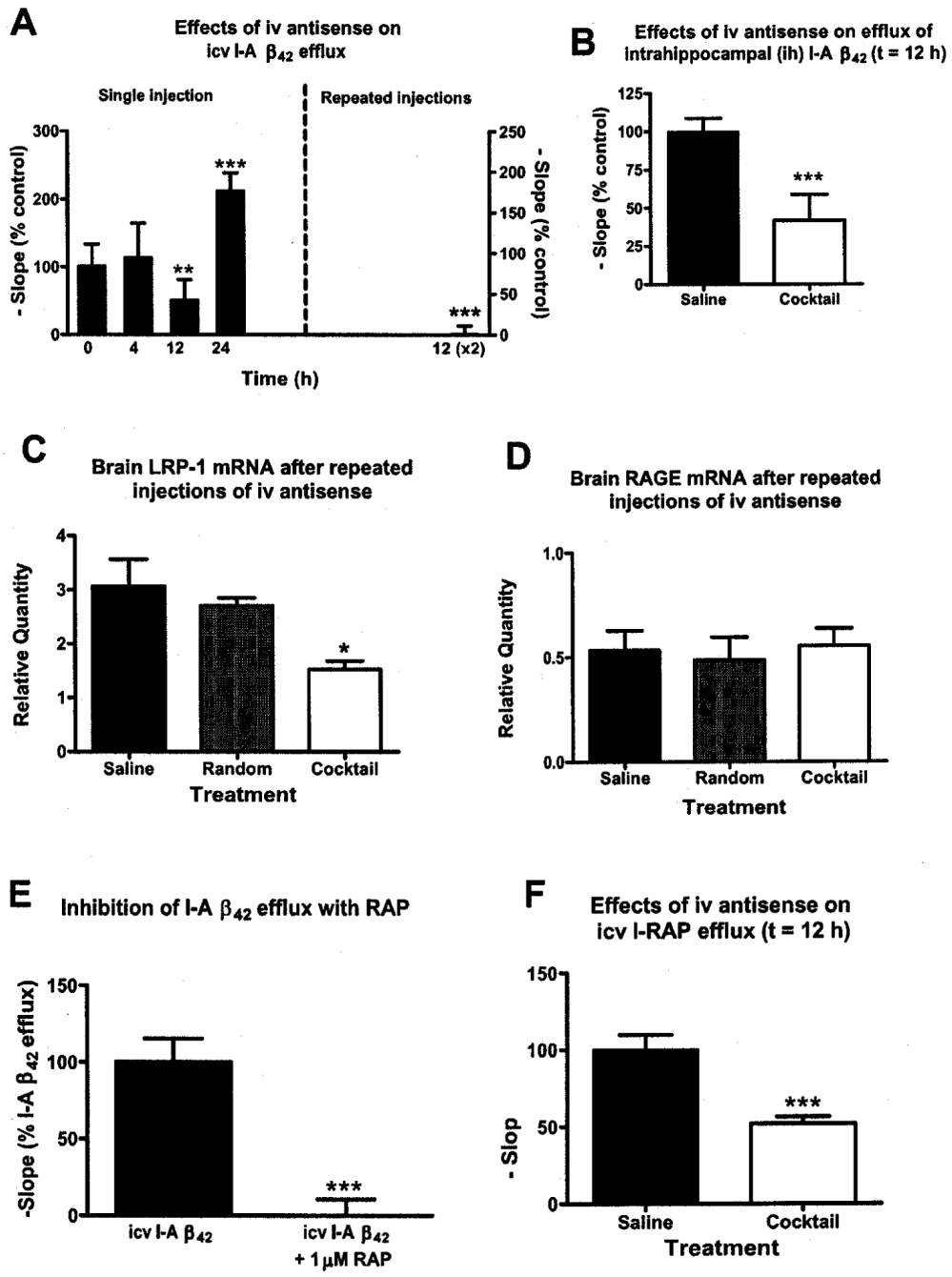

Fig. 3.

Effects of i.v. administered cocktail in Cd-1 mice. (**A**) A single i.v. injection of antisense cocktail (7 μg) comparedo to saline significantly impaired brain efflux of I-Aβ_{42} at t = 12 h with significant rebound by 24 h (n = 11–14/group). Mice that received a second i.v. injection of cocktail 12 h after the first (right side of graph, n = 11) showed a near total impairment in I-Aβ_{42} efflux 24 h after the first injection. (**B**) IV cocktail also impaired efflux of I-Aβ_{42} injected into the hippocampus (n = 13/group). Mice given the double injection of IV cocktail had (**C**) decreased brain mRNA for LRP but (**D**) not of RAGE (n = 4/group for b-c). (**E**) Demonstrates that RAP inhibits brain efflux of i.c.v. administered I-Aβ_{42} as expected for this known LRP-1 substrate (n = 9/group). (**F**) Inhibition of LRP-1 activity with antisense cocktail is confirmed

by its ability to inhibit efflux of I-RAP ($n = 13$). For all figures, data shown as mean +/− SEM, except (**A**) which shows SD. * = $p < 0.005$, ** = $p < 0.01$, * * * = $p < 0.001$.

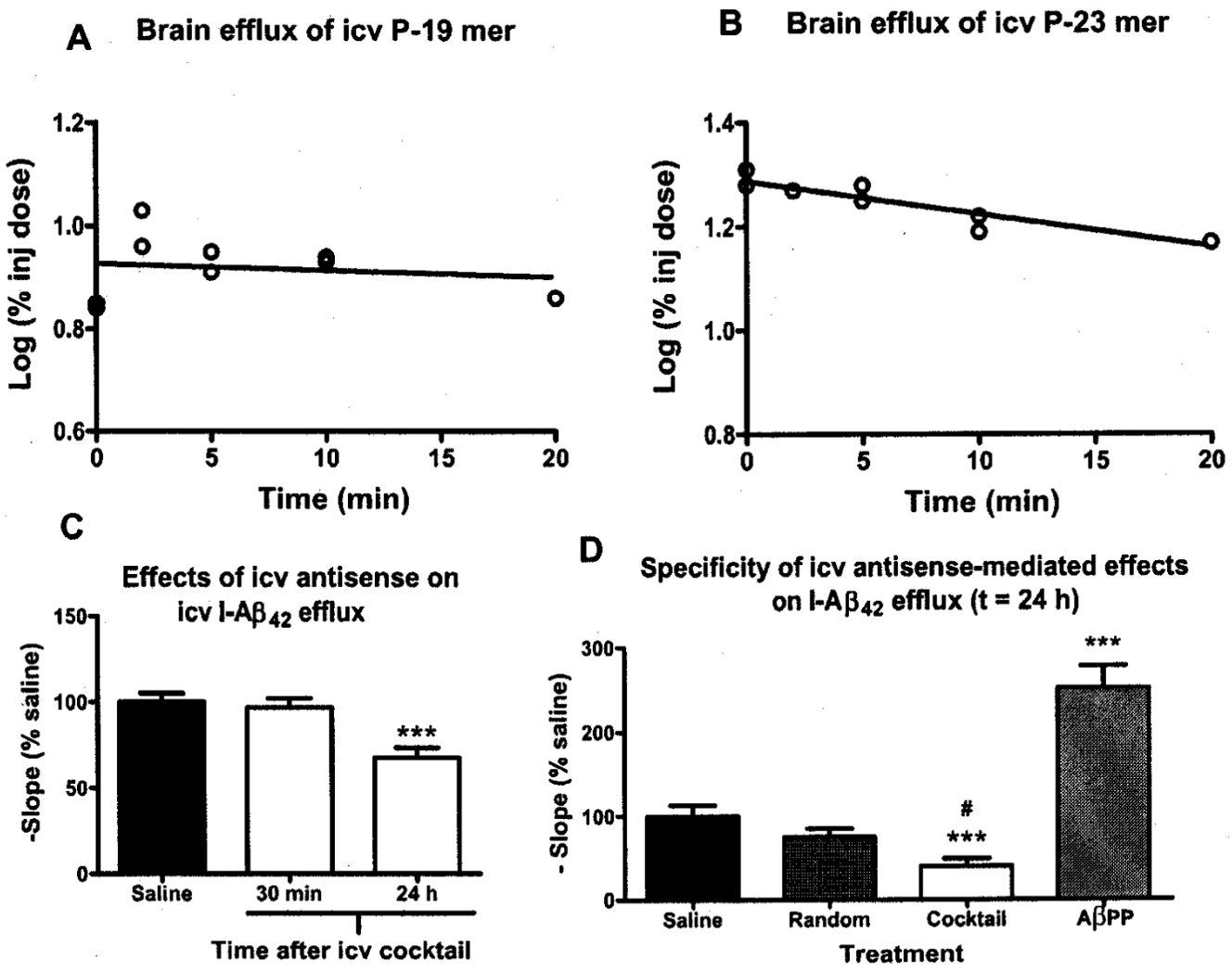

Fig. 4.

Effects of acute i.c.v. cocktail administration. **(A-B)** Brain efflux of i.c.v. **(A)** P-19 mer and **(B)** P-23 mer antisense cocktail PS-ODNs. The slope of the line represents the rate of brain efflux which was 0.0013% and 0.0063% of the injected dose/min for the P-19 mer and P-23 mer, respectively (n = 2–3 mice/time point). **(C)** Single injection of i.c.v. antisense cocktail (200 ng dose) significantly impaired I-Aβ_{42} efflux at t = 24 h, but not at t = 30 min (n = 12–15/group). * * * = $p < 0.001$. **(D)** Treatment with i.c.v. antisense cocktail produced a significant decrease in I-Aβ_{42} efflux compared to saline (* * * = $p < 0.0001$) and random (# = $p < 0.05$) antisense treated mice. Treatment with i.c.v. AβPP antisense produced a significant increase in I-Aβ_{42} efflux compared to saline treated mice. (n = 15–17/group). For all panels, data shown as mean +/− SEM.

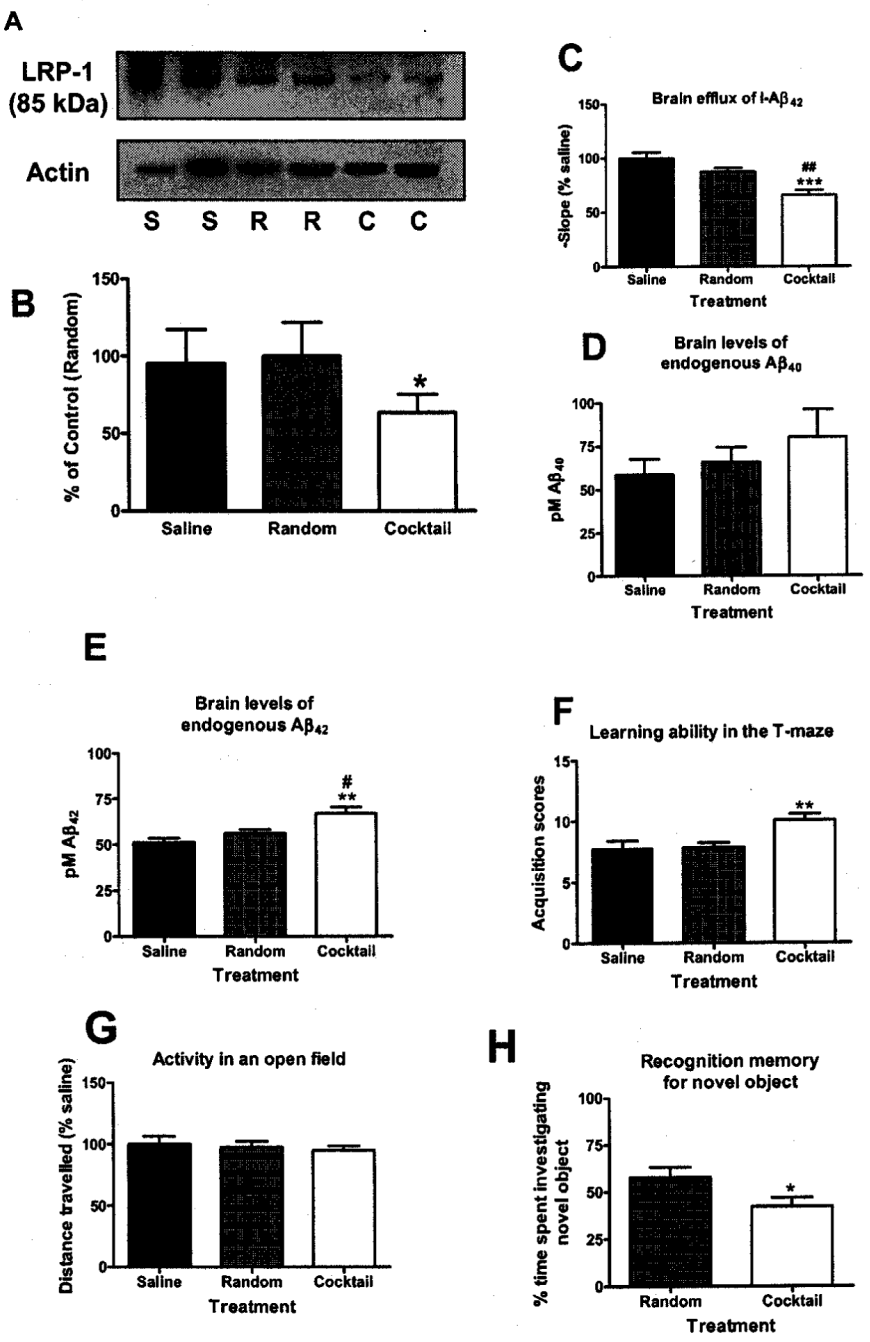

Fig. 5.

Effects of chronic (1 week) ICV cocktail infusion (100 ng/h) on I-Aβ_{42} efflux, brain levels of Aβ_{40} and Aβ_{42}, learning ability, recognition memory and brain levels of LRP-1 protein in mice. (**A**) Western blot for small (85 kDa) subunit of LRP-1 shows that mice treated with antisense cocktail ("C") demonstrated significantly less band intensity in brain homogenates compared to random ("R") or saline ("S") treatments, *$p < 0.05$). (**B**) For optical density graphs, $n = 4$ bands/bar). (**C**) Infusion of cocktail but no random antisense significantly decreased brain efflux of I-Aβ_{42}. ($n = 12$–16/group). ## = $p < 0.01$ vs cocktail, *** = $p < 0.0001$ vs saline. (**D**) Aβ_{42}, but not (**E**) Aβ_{40}, was significantly increased in brain homogenate as assessed by ELISA ($n = 5$–6/group #$p < 0.05$ vs random, **$p < 0.01$ vs saline. (**F**) Cocktail impaired learning

in the active avoidance T-maze (**G**) without affecting the potential confounder of activity (n = 12–15/group, $^{**}p < 0.01$. (**H**) The novel object recognition test demonstrated that cocktail induced a significant deficit in recognition memory compared to random treated mice. (n = 11–17/group, $^{*}p < 0.05$. Data shown as mean +/− SEM.

Table 1

Comparison of Pharmacokinetics of IV P-Olg for target and non-target tissues *in vivo*. Percent of injected dose taken up per g of liver or brain for P-19mer and P-23mer 5, 10, and 30 min after i.v. injection; n = number/group

	Brain (n)	Liver (n)
P-19mer		
5 min	0.042 (2)	4.47 (3)
10 min	0.079 (3)	5.54 (3)
30 min	0.116 (3)	10.4 (3)
P-23mer		
5 min	0.010 (3)	2.71 (3)
10 min	0.044 (3)	5.33 (3)
30 min	0.052 (3)	7.67 (3)